Raman Scattering Enhancement by Optical Confinement in a Semiconductor Planar Microcavity

A. Fainstein and B. Jusserand
France Telecom/CNET/PAB-Laboratoire de Bagneux, B.P. 107, 92225 Bagneux Cedex, France

V. Thierry-Mieg
Laboratoire de Microstructures et de Microélectronique/Centre National de la Recherche Scientifique, B.P. 107, 92225 Bagneux Cedex, France
(Received 1 June 1995)

We report optical-phonon Raman scattering enhancements of over 4 orders of magnitude in a $\lambda/2$ semiconductor planar microcavity. By varying the incidence angle both excitation and Stokes photons can simultaneously resonate with the cavity mode, their fields being strongly amplified. We demonstrate the cavity geometry as a promising tool to study solid state excitations in reduced dimensions with highly increased sensitivity.

PACS numbers: 78.30.Fs, 42.50.–p, 42.82.Et, 78.66.Fd

Spontaneous emission is not an intrinsic property of an atom but of the coupled atom-vacuum-field system. The radiation characteristics of an atom can be altered by modifying the vacuum field fluctuations in its vicinity, e.g., by placing it near a surface [1] or within a microcavity [2,3] or a photonic band-gap material [4]. In particular, the decay of the excited atom into a definite photon mode can be strongly enhanced (inhibited) by placing it in maxima (minima) of the photon field spatial distribution [5]. Besides, an increase of spontaneous and stimulated emission by enhancement of the light field at the *excitation* energy has been reported [6]. Thus, modifications of the electric fields can be exploited in both first order in light-matter interaction processes: emission *and* absorption. By the same token, a strong enhancement or inhibition of the Raman cross section of an active material embedded in a cavity may be envisaged through the modification of its two vertexes of light-matter interaction. In fact, enhancement of inelastic scattering has been observed in micrometer-size droplets which act as an optical cavity [7–9]. Also, field confinement effects at the Stokes energy have been observed for liquid benzene in a piezoelectrically controlled microcavity [10].

In this Letter we report an investigation of Raman scattering in a monolithic GaAs/AlAs based half-wave planar microcavity. A double-resonant condition controlled by the incident angle has been achieved, in which *both* the excitation and Stokes photons couple to cavity modes leading to a dramatic increase of the optical-phonon Raman signals. We show that these signals arise from the "interface-phonon" band of the cavity as a whole, with discrete peaks due to finite size effects.

In order to increase the microcavity Q value, and thus the electric field enhancement, high reflectivity mirrors must be used. Although this implies no limitation for luminescence studies, in which the excitation is made at energies above the cavity stop band, it poses a problem for Raman experiments were photons differing by the energy of the excitation under study must get into, or go out from, the microcavity. The experiments reported in Ref. 10 relied on a cavity-single-resonance condition: only the bottom mirror of the piezoelectrically controlled cavity was reflecting at the excitation energy so that *only* the Stokes radiation was confined. The stimulated Raman scattering studies on droplets cited above [7–9], on the other hand, made use of relatively large cavity diameters (10–30 μm) and thus high mode densities enabling the tuning of laser energy (or droplet size) so that cavity double resonance was possible.

For a $\lambda/2$ semiconductor microcavity only one cavity vertical mode is available, and the two Bragg reflectors are efficient, for both excitation and Stokes photons. However, we show that both photons can be coupled simultaneously to the cavity by tuning their propagation angle with respect to the cavity axis, z. In fact, if a photon propagating along z resonates (i.e., couples to a vertical cavity mode) at an energy ω_s, one incident at an angle θ_0 (measured in air) will resonate at a *larger* energy given approximately by

$$\omega_i \approx \omega_s / \cos(\theta_0 / n_{\text{eff}}), \tag{1}$$

where n_{eff} is the structure effective refractive index. When $\omega_i - \omega_s$ equals an excitation of the system, the conditions for the observation of "geometrical" double-resonant Raman scattering are obtained.

Our microcavity (inset of Fig. 1) consists [11] of a half-wave AlAs spacer enclosed by GaAs/AlAs quarter-wave layers (13.5 pairs above, 20 below) acting as distributed Bragg reflectors (DBR's), grown by molecular beam epitaxy on a GaAs wafer. Two 12-nm-wide strained $In_{0.14}Ga_{0.86}As$ quantum wells are located at the center of the AlAs cavity, each enclosed by 1-nm-wide layers of GaAs. A finesse of 300 was estimated from reflectivity curves [11]. The thickness of all layers is largest at the center of the wafer enabling the tuning of the cavity mode by displacing radially the spot under examination. For

 0031-9007/95/75(20)/3764(4)$06.00 © 1995 The American Physical Society

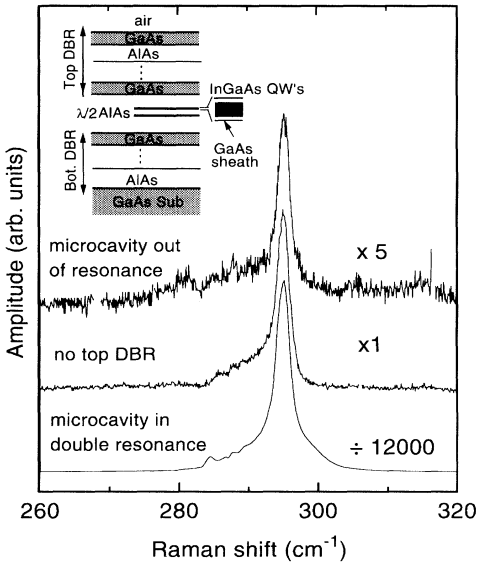

FIG. 1. Raman spectra taken with $z'(x,y)\bar{z}$ configuration for both the cavity and test (without top DBR) samples. z' corresponds to the laser incident at 54° respect to z (external to the sample). The laser energy was 1.37 eV, below the QW's exciton. A sketch of the cavity sample is shown in the inset.

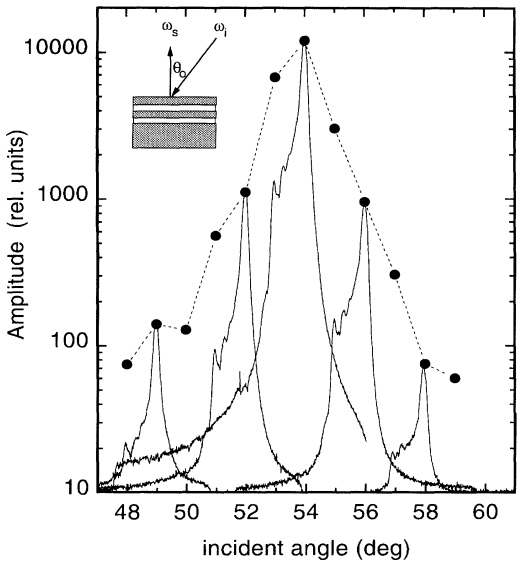

FIG. 2. Dependence of the Raman scattering amplitude normalized to the test sample (full dots) on θ_0 (measured external to the sample). The cavity is tuned along z to the LO Stokes energy. The dashed line is only a guide to the eye. Raman spectra are shown at a few different angles for illustration, shifted so that the LO peak coincides with the respective angle. The inset shows the scattering configuration.

comparison, a second sample identical to the first but with its growth stopped just after the AlAs cavity (i.e., without top DBR) was also studied.

Raman experiments were performed at 77 K. The scattered radiation was collected along the cavity axis (with a $f/2$ aperture), while the incident laser angle was free to vary (inset in Fig. 2). Figure 1 shows Raman spectra of both the cavity and test samples, taken for crossed $z'(x,y)\bar{z}$ configuration at 1.37 eV [below the quantum well (QW) gap $\approx$1.385 eV]. z' indicates light incident, for this case, at 54° (external) with respect to z. For the lower spectrum θ_0 and the spot under observation are such that both Stokes and excitation photons are simultaneously resonant to the cavity mode and differ in energy by the longitudinal optical phonon of GaAs (LO $\approx$ 295 cm^{-1}). The uppermost spectrum was taken with the same incident angle but with the spot displaced so that the cavity was completely detuned. Note the difference in amplitude between the spectra: enormous scattering enhancement and inhibition respect to the test sample are obtained by cavity optical confinement. The power dependence of the spectra is linear up to 100 mW (for a laser spot of $\approx$100 μm), indicating a spontaneous Raman process.

We have evaluated the field distribution within the heterostructures by the standard method of matrices [12]. For the $\lambda/2$ AlAs cavity the electric field amplitude is enhanced throughout the whole structure, displaying a maximum of about 20 at the center (with respect to the free space value). For the sample without top DBR, on the contrary, the electric field decays exponentially into the bottom mirror. We recall here that the Raman efficiency contains two (squared) matrix elements of light-matter interaction proportional to the electric field amplitude, due to the incoming and outgoing photon vertexes [13]. Thus, if these amplitudes are enhanced, the Raman scattering efficiency should be fourth order in the enhancement factor.

Assuming that the Raman spectra shown in Fig. 1 are exclusively due to the QW's GaAs-like phonons [14], the calculated cavity enhancement factor explains consistenly the 4 orders of magnitude difference between the Raman intensity of the samples with and without top DBR. Nevertheless, this is only an approximation because for the double-resonance condition photons of the two energies can traverse throughout the complete structure. Consequently, phonons in the whole sample are likely to participate in the enhanced scattering, as will be discussed below.

The Raman enhancement in a planar microcavity is critically sensitive on the incidence angle θ_0. This is shown in Fig. 2 where we present the scattering intensity as a function of θ_0 for a fixed laser energy and with the cavity mode along z in resonance with the LO-phonon Stokes frequency. More than 2 orders of magnitude variations of the Raman amplitude are observed by rotating the incident angle less than 4°, thus going from double to single resonance. The angular dependent half width at half maximum (HWHM) is of the order of 1°, which is consistent [as estimated from Eq. (1)] with the measured reflectivity peak HWHM in the same structure (0.3 nm) [11].

For highlighting peaks other than the LO phonon, one has simply to tune the cavity mode with the desired Stokes

energy and vary the angle for double resonance. In fact, by doing this peaks that appear secondary in Figs. 1 and 2 can be made even larger than the LO peak. We may visualize this selective enhancement by recording spectra for different spot positions (i.e., the cavity mode resonant with *different* Stokes energies) but leaving the angle fixed. By doing this we slightly detune the laser photons, but taking advantage of the width of the geometrical resonance double resonance is almost preserved. This is shown in Fig. 3, for $\theta_0 = 53°$ (corresponding to double resonance slightly below the LO-phonon Stokes energy). The spectrum for 20.62 mm is similar to the ones shown above. On the other hand, all secondary structures are amplified by displacing the cavity mode through the Stokes region, from $\approx$304 in the lower spectrum to $\approx$ 278 cm^{-1} in the upper one.

We have discussed up to this point general features of Raman scattering in a planar cavity geometry, e.g., the concept of geometrical double resonant enhancement and, in particular, the cavity mode and angular tuning for selective amplification of different signals. We turn now to the analysis of our specific Raman spectra. Some general conclusions can be drawn from the data: (i) the Raman signals are mainly between the TO (transverse optic phonon, $\approx$272 cm^{-1}) and LO frequencies of bulk GaAs; (ii) two bands can be identified according to their intensity, one very strong and delimited by the LO phonon and a second peak at $\approx$285 cm^{-1} (see the spectrum for 20.68 mm in Fig. 3), the other much weaker between the latter and the TO frequency; (iii) the most intense peaks occur at the LO phonon and at $\approx$285 cm^{-1}, several smaller ones appearing between them; and, finally, (iv) scattering occurs principally for $z'(x, y)\bar{z}$ configuration, corresponding to deformation potential mediated scattering by phonons of $B_2(z)$ symmetry [13].

The above features reflect optical phonon scattering likely to be due to the so-called upper interface-phonon band of layered GaAs which extends, with details depending on the GaAs/AlAs width ratio, between the LO and the midpoint between the LO and TO [15]. We assign the observation of several peaks instead of a continuous band to finite size effects (i.e., to the discretization of k_z due to the lack of periodicity along z) as discussed theoretically by Camley and Mills [16] and observed by Pinczuk *et al.* [17] in the context of plasmons in layered electron gases.

Figure 4 shows our structure GaAs-like optical-phonon dispersion as a function of in-plane wave vector k (dotted lines). The curves were calculated extending the approach of Camley and Mills [16] to heterostructures with an arbitrary sequence of layers (here the cavity is limited by air and substrate) by the use of a matrix method similar to that used to describe the propagation of light in layered media [12]. We describe the optical phonons of the 12-nm InGaAs QW's plus their 1-nm GaAs caps as those of 14-nm-thick GaAs slabs. In fact, due to a compensation of the effects of alloying and strain, the zone center GaAs-like phonons of thin strained $In_xGa_{1-x}As$ layers grown on GaAs resemble almost exactly those of GaAs [14]. Moreover, we ignore retardation effects and also mechanical boundary conditions at the GaAs interfaces. The latter are known to be important to describe the coupling of "interface" and confined phonon modes in thin QW's. Here the high-order confined LO modes, which could also lead to scattering below the LO frequency [15], should not be resolved due to the relatively large thickness of the GaAs layers (14 nm for the QW's, $\approx$63 nm for the

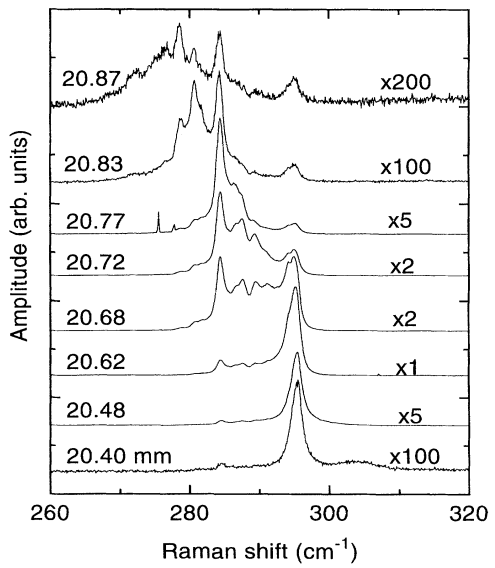

FIG. 3. Raman scattering spectra for different positions in the wafer, i.e., with selective enhancement of different parts of the Stokes region. The incident angle was held fixed, for exact double resonance slightly below the LO phonon.

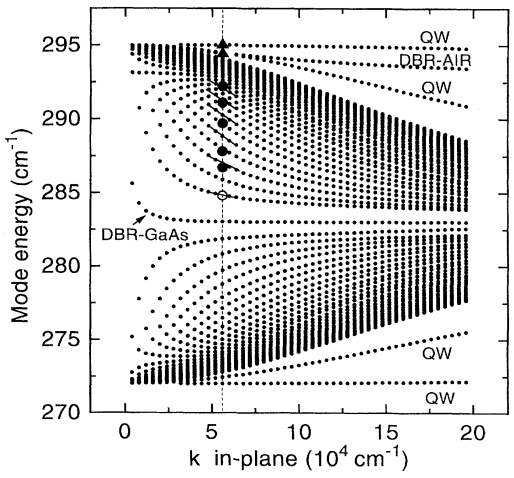

FIG. 4. Calculated optical phonon dispersion as a function of in-plane wave vector k (dotted lines). The vertical dashed line denotes the experimental transfered in-plane k. Triangles and open circles indicate the measured frequency of the most intense peaks. Full circles correspond to the observed smaller structures. The short solid lines indicate the modes expected to scatter due to parity.

DBR's). One mode appears for each interface, contributing to two almost continuous bands and clearly separated "surface modes" [16]. The two bands in Fig. 4 originate from the DBR's, and are discretized by their finite size. Each discrete curve corresponds to a different quantized wave vector along z: if D and d are the total size of the structure and the DBR's period, respectively, for the upper band k_z ranges from the smallest value (π/D) at the bottom to the largest possible one (π/d) at the top. The modes which appear separated from these two bands arise from the QW's and from the surfaces which bound the DBR's. Thus, scattering from specific modes may provide a probe on the field distribution within the structure.

Among the large number of branches in Fig. 4 only a few are expected to have a significant contribution in our experiment. First, the modes in the upper (lower) half of Fig. 4 are mainly polarized along z (k). Thus, the observation of intense scattering only between the LO frequency and 285 cm^{-1} follows from the selection rules which for $z'(x,y)\bar{z}$ configuration correspond to z-polarized $B_2(z)$ symmetry phonons [13]. Second, in a cavity photons are multiply reflected due to the DBR's leading to forward scattering (FS) events in addition to normal backscattering (BS). For both, the *in-plane* transferred k is the same (denoted for our experiment by the vertical line in Fig. 4). In FS, the total transferred wave vector is mainly perpendicular to z (i.e., $k_z \approx 0$). In BS, on the other hand, it is mostly along z [15].

The Raman spectra consist of two main peaks, one at $\approx$285 cm^{-1} (open circle in Fig. 4) and one, with some doublet structure, around 295 cm^{-1} (triangles in Fig. 4). We assign the latter to scattering by the QW's modes. These are independent of k_z and thus couple to both FS and BS processes indistinctly. Concerning the peak at 285 cm^{-1}, we assign it to FS and BS by the bottom mode of the DBR's upper band, which corresponds to $k_z \approx 0$. In fact, for BS at cavity double resonance $k_z = 2\pi/d$ (by construction of the DBR's). This wave vector is equivalent to zero [15]. In addition to the precise accord between theory and experiment without any adjustable parameter (see Fig. 4), these assignments are further supported by similar agreement obtained in different microcavity structures. We assign the smaller peaks that appear between the LO and 285 cm^{-1} (full circles in Fig. 4) to scattering by modes *within* the DBR's upper band, due to k_z nonconserving processes [17]. The experimental peaks are reasonably well accounted for by theory (within 1 cm^{-1}) only if one in every two modes scatter. This reflects a parity selection rule: Since the photon field distribution is even respect to the center of the cavity, scattering only by modes with an even associated polarization (marked with solid lines in Fig. 4) is allowed. The signal coming from the QW's and the DBR's thus appear in essentially separate energy ranges. Hence, the 4 orders of magnitude enhancement shown in Fig. 1 does indeed reflect the field amplification in the center of the cavity.

In conclusion, we have observed optical-phonon scattering originating from the interface-phonon band of the microcavity, discretized by finite size effects. We have shown that the Raman scattering process is sensitive to the electric field amplitude modifications in optical microstructures and, in particular, that its efficiency may be strongly enhanced or inhibited by a microcavity structure. A direct parallel of the observed geometrically enhanced scattering can be made with the well-known electronic resonant Raman processes [13]. As for the latter, which is used both to enhance otherwise subtle processes and, conversely if the scattering is well understood, to study the electronic band structure, the enhancement or inhibition of Raman efficiency in microcavities can be used both to amplify weak processes and, conversely by using a well known active material, to characterize the internal field distribution within photonic microstructures. These results open promising ways to study weakly scattering objects, such as single interfaces and quantum dots.

We are pleased to aknowledge I. Abram, M. Bensoussan, J. Y. Marzin, J. L. Oudar, R. Planel, and B. Sermage for numerous helpful discussions. I. A. and B. S. provided us with well characterized samples, designed by I. A., and unpublished results on them. A. F. thanks the Fundación Antorchas for financial support.

[1] R. E. Kunz and W. Lukosz, Phys. Rev. B **21**, 4814 (1980).
[2] See, for instance, R. J. Thompson *et al.*, Phys. Rev. Lett. **68**, 1132 (1992).
[3] For a review, see Y. Yamamoto and R. E. Slusher, Phys. Today **46**, 66 (1993); R. E. Slusher and C. Weisbuch, Solid State Commun. **92**, 149 (1994).
[4] E. Yablonovitch, Phys. Rev. Lett. **58**, 2059 (1987).
[5] See, for instance, Z. L. Zhang *et al.*, Appl. Phys. Lett. **64**, 1068 (1994).
[6] F. De Martini *et al.*, Opt. Lett. **17**, 1370 (1992).
[7] J. B. Snow *et al.*, Opt. Lett. **10**, 37 (1985).
[8] Shi-Xiong Qian and Richard K. Chang, Phys. Rev. Lett. **56**, 926 (1986).
[9] H.-B. Lin *et al.*, Opt. Lett. **17**, 828 (1992).
[10] F. Cairo *et al.*, Phys. Rev. Lett. **70**, 1413 (1993).
[11] This structure was studied by I. Abram *et al.*, Appl. Phys. Lett. **65**, 2516 (1994).
[12] A. Yariv and P. Yeh, in *Optical Waves in Crystals* (Wiley, New York, 1984).
[13] M. Cardona, in *Light Scattering in Solids,* edited by M. Cardona and G. Güntherodt (Springer, Berlin, 1982), Vol. 2.
[14] See, for instance, F. Iikawa *et al.*, Solid State Commun. **68**, 211 (1988).
[15] B. Jusserand and M. Cardona, in *Light Scattering in Solids,* edited by M. Cardona and G. Güntherodt (Springer, Berlin, 1989), Vol. 5.
[16] R. E. Camley and D. L. Mills, Phys. Rev. B **29**, 1695 (1984).
[17] A. Pinczuk *et al.*, Phys. Rev. Lett. **56**, 2092 (1986).